J. Hydrol. Hydromech., 66, 2018, 3, 330–336
DOI: 10.2478/johh-2018-0012

Laboratory testing of granular kinetic theory for intense bed load transport

Václav Matoušek*, Štěpán Zrostlík

Czech Technical University in Prague, Department of Civil Engineering, Thákurova 7, 166 29 Prague 6, Czech Republic.
* Corresponding author. E-mail: v.matousek@fsv.cvut.cz

Abstract: Collisional interactions in a sheared granular body are typical for intense bed load transport and they significantly affect behavior of flow carrying bed load grains. Collisional mechanisms are poorly understood and modelling approaches seldom accurately describe reality. One of the used approaches is the kinetic theory of granular flows. It offers constitutive relations for local shear-induced collision-based granular quantities – normal stress, shear stress and fluctuation energy – and relates them with local grain concentration and velocity. Depth distributions of the local granular quantities produced by these constitutive relations have not been sufficiently verified by experiment for the condition of intense bed load transport in open channels and pressurized pipes. In this paper, results from a tilting-flume facility including measured velocity distribution and deduced concentration distribution (approximated as linear profiles) are used to calculate distributions of the collision-based quantities by the constitutive relations and hence to test the ability of the kinetic-theory constitutive relations to predict conditions observed in these collision-dominated flows. This test indicates that the constitutive relations can be successfully applied to model the local collisional transport of solids at positions where the local concentration is not lower than approximately 0.18 and not higher than approximately 0.47.

Keywords: Granular flow; Sheet flow; Sediment transport; Grain collision; Tilting flume experiment.

INTRODUCTION

Coarse granular flows carry grains which tend to intensely interact with each other. Depending on the flow conditions, the interactions take the form of either collisions or sliding contact. Typically, the flows tend to form a layered structure composed of a sliding layer in which grains are in virtually permanent contact and of a collisional transport layer in which conveyed grains suffer intense mutual collisions. Examples are coarse slurry flows near the deposition-limit velocity in pressurized pipes (the sliding layer may dominate) or flows with intense transport of coarse sediment in steep-slope mobile-bed streams (the collisional layer dominates). Appropriate modelling of friction and transport conditions is crucial for models predicting the slope of the energy grade line and solids carrying capacity of such flows. Modelling approaches are based either on an employment of integral quantities of the flow or else based on local quantities associated with the internal structure of the flow. In our earlier work, we followed the integral-quantity approach and made suggestions for modelling of solids transport and bed friction in the upper-plane bed regime in pipes and open channels (Matoušek et al., 2013, 2016a).

The sliding mechanism in a granular body is relatively well understood and successfully applied, for instance, in two-layer models of stratified flows in pressurized pipes. The collisional mechanism, however, is much more complex and requires an analysis of relevant quantities at a local level in the flow. Bagnold's pioneering work (Bagnold, 1954) on local granular rheology of solid-liquid mixtures was carried out for very specific conditions and its results do not seem to be directly applicable to collisional flows transporting grains of density different from the carrier density in open channels (Armanini et al., 2005; Hunt et al., 2002) or pipes. It seems more appropriate to base modelling of flows dominated by granular collisions on kinetic theory of granular flows. Kinetic-theory based models are able to predict a layered pattern of the flow and values of relevant flow quantities (Berzi and Fraccarollo, 2013; Capart and Fraccarollo, 2011). Model predictions include integral flow quantities (discharges of solids and mixture, flow depth) and simplified distributions of solids concentration and velocity. Typically, a kinetic-theory based model assumes certain granular-rheological related conditions at flow interfaces and quantifies the interfacial stresses, concentration, and velocity. Additional equations (momentum balances) are employed to use the interfacial granular quantities for the prediction of thicknesses of the relevant layers. The discharges of solids and mixture are obtained through integration of the velocities and concentrations over the flow depth. The aim of this paper is to employ results of our previous experiments (which include distributions of velocity and concentration) to shed light on the distribution of granular quantities by the constitutive relations within the collisional layer and its consequences for the application of the constitutive relations in this layer for which a big difference in local concentrations at the top and at the bottom of the layer is typical.

MODELLING OF DISTRIBUTIONS IN A COLLISIONAL LAYER

It is typical for the discussed flows that local concentrations and velocities of the grains span a broad range of values over the thickness of the collisional layer. Associated local granular stresses vary considerably with local position within this collisional layer as well.

Kinetic theory of granular flows

Classical kinetic theory (CKT) considers sheared granular bodies, in which grains are supported exclusively by mutual binary collisions. Constitutive relations are formulated for local grain stresses (both normal and shear stresses) and for a kinetic-theory based balance of grain fluctuation energy in the collisional regime.

CKT covers collision-driven transport of grains at low to moderate local concentrations where the granular motions can be considered as uncorrelated. Recently, the kinetic theory was extended (the extended kinetic theory EKT) to also cover correlated motion of grains at high local concentrations. In principle,

EKT modifies the constitutive relations for the condition of the local concentration $c \rightarrow 1$, which a purely theoretical limit as the local concentration of sediment grains hardly exceeds 0.65. The condition is called the dense limit. So far, most kinetic-theory based models for contact-load transport have only considered the uncorrelated grain condition above the base of the deposit (Armanini et al., 2005; Capart and Fraccarollo, 2011; Jenkins and Hanes, 1998; Spinewine and Capart, 2013), only a few models have employed the dense limit using the EKT principle (Berzi, 2011; Berzi and Fraccarollo, 2013).

Principles of granular rheology in kinetic theory

In the kinetic theory of granular flows, the local shear-induced granular normal stress (also called granular pressure in the literature), σ_s, is related to the local concentration of grains, c, and to the local granular temperature, T. This temperature T expresses a measure of local grain velocity fluctuations due to intergranular collisions. A determination of the local T is one of the main challenges associated with an application of the kinetic theory. The local shear induced granular shear stress, τ_s, is also related to c and T at any vertical position y above the bed. Moreover, τ_s is related to the local strain rate γ, i.e. the distribution of u ($\gamma = \mathrm{d}u/\mathrm{d}y$, u = local longitudinal velocity of grains). The kinetic theory introduces the coefficient of wet restitution, e, as an additional parameter affecting the stresses at the local level. Some kinetic theory based models consider $e = 1$ for convenience. Relations based on CKT do not contain any empirical constants. EKT-relations introduce one empirical constant described below.

Constitutive relations

The general forms of the kinetic theory based relations for the local granular normal stress, σ_s, and the granular shear stress, τ_s, due to intergranular contacts read respectively

$$\sigma_s = 4 \cdot \rho_s \cdot f_\sigma \cdot c \cdot G \cdot T \tag{1}$$

$$\tau_s = \rho_s \cdot f_\tau \cdot c \cdot G \cdot \sqrt{T} \cdot \gamma \cdot d \tag{2}$$

In Equations 1 and 2, ρ_s = density of grains, d = grain size, G, f_σ, f_τ = concentration-related functions. Besides the local concentration c, both stresses depend on the granular temperature T, the shear stress is further dependent on the strain rate γ.

In CKT, the concentration-related function

$$G = c \cdot g_0 = c \cdot \frac{2 - c}{2 \cdot (1 - c)^3} \tag{3}$$

where g_0 = radial distribution function at contact. Relations for functions f_σ and f_τ take different forms in different models in the literature, the most general being those considering e differing from 1,

$$f_\sigma = \frac{1 + e}{2} + \frac{1}{4 \cdot G} \tag{4}$$

$$f_\tau = \frac{8}{5 \cdot \sqrt{\pi}} \cdot \left(\frac{1 + e}{2} + \frac{\pi}{32} \cdot \frac{\left[5 + 2 \cdot (1 + e) \cdot (3 \cdot e - 1) \cdot G\right] \cdot \left[5 + 4 \cdot (1 + e) \cdot G\right]}{\left[24 - 6 \cdot (1 - e)^2 - 5 \cdot \left(1 - e^2\right)\right] \cdot G^2} \right) \tag{5}$$

If the assumption of the dense limit in EKT is taken, then $1/G \rightarrow 0$ at $c \rightarrow 1$ and the functions f_σ and f_τ reduce (for the condition $1/G = 0$) to

$$f_\sigma = \frac{1 + e}{2} \tag{6}$$

$$f_\tau = \frac{8}{5 \cdot \sqrt{\pi}} \cdot \left(\frac{1 + e}{2} + \frac{\pi}{4} \cdot \frac{(3 \cdot e - 1) \cdot (1 + e)^2}{24 - (1 - e) \cdot (11 - e)} \right) \tag{7}$$

while the G-function expands (because of the g_0-function expansion) to

$$G = c \cdot \frac{2 - c_f}{2 \cdot \left(1 - c_f\right)^3} \cdot \frac{c_c - c_f}{c_c - c} \tag{8}$$

for $c_f \le c \le c_c$, where c_f = freezing concentration and c_c = random close packing concentration (Torquato, 1995).

Defining the granular viscosity as $\eta_s = \tau_s / \gamma$, a local value of η_s is related to local values of the restitution coefficient e, concentration c, and granular temperature T by, $\eta_s = \rho_s \cdot f_\tau \cdot c \cdot G \cdot \sqrt{T} \cdot d$. Another constitutive relation expresses the balance of the particle collisional fluctuation energy. It requires that the gradient of the vertical component of the flux of particle fluctuation energy, Q, balances the net rate of production of fluctuation energy per unit volume of the mixture (Jenkins and Hanes, 1998),

$$-\frac{\partial Q}{\partial y} + \tau_s \cdot \gamma - \frac{24}{\sqrt{\pi}} \cdot \rho_s \cdot c \cdot G \cdot (1 - e) \cdot \frac{\sqrt{T^3}}{d} = 0 \tag{9}$$

The first term on the left-hand side of Equation 9 represents the diffusion of fluctuation energy, the second term the production of energy due to shearing, and the third term represents the rate of collisional dissipation, i.e. the fluctuation energy dissipated by interparticle collisions (Armanini et al., 2005). The flux Q is

$$Q = -\frac{4}{\sqrt{\pi}} \cdot \rho_s \cdot f_Q \cdot c \cdot G \cdot \sqrt{T} \cdot \frac{\partial T}{\partial y} \cdot d \tag{10}$$

in which the function f_Q reads

$$f_Q = 1 + \frac{9 \cdot \pi}{32} \cdot \left(1 + \frac{5 \cdot \pi}{12 \cdot G}\right)^2 \tag{11}$$

and in the dense limit $f_Q = 1 + \frac{9 \cdot \pi}{32}$.

EKT handles the problem of one limiting concentration ($1/G \rightarrow 0$, i.e. $c \rightarrow 1$). This problem is relevant to bed load transport as local concentrations near the top of the bed may reach high values of c, although they tend to the bed concentration c_b ($c \rightarrow c_b$, typically $c_b = 0.6$) rather than $c \rightarrow 1$. The bed concentration is affected by the grain shape for instance and may reach c_c as a limit. EKT also employs the dimensionless correlation length L (e.g. Berzi, 2011) as a parameter quantifying the effect of the presence of correlated motion of grains on the collisional energy dissipation,

$$L = \frac{C \cdot \sqrt[3]{G} \cdot \gamma \cdot d}{2 \cdot \sqrt{T}} \tag{12}$$

in which C = material constant of order unity. At any position y within the collisional layer, $L(y) \leq L_{max}$ where $L_{max} = 1$ (Berzi, 2011).

An application of the kinetic theory in the bed load transport also encounters a problem of another limiting concentration, namely $c \rightarrow 0$ typical for the region near the top of the collisional layer. At the top of the layer, $c = 0$ and the granular stresses are zero too. The function $G = 0$ and hence both f_σ, f_τ tend to infinity at the top of the layer. It follows that there must be some non-zero minimum local concentration required to establish the collisional condition expected by the classical kinetic theory.

Momentum balance equations

Alternative equations relating the distribution of the local concentration with the distributions of the granular stresses are based on the principle of momentum balance. In gravity-driven solid-liquid flow with a free surface, the force balance between the driving force and the resisting force assumes that the total shear stress, τ_e (composed of the granular component, τ_s, and the liquid component, τ_f) at each vertical position y balances the longitudinal component of the weight of overlaying burden of liquid and solids,

$$\tau_e = \tau_s + \tau_f = g \cdot \sin\omega \cdot \int_y^H \left[\rho_s \cdot c + \rho_f \cdot (1-c)\right] \cdot dy \qquad (13)$$

in which ρ_f = density of liquid, g = gravitational acceleration, ω = angle of longitudinal slope, and H = total flow depth. The granular component of the total shear stress

$$\tau_s = \rho_s \cdot g \cdot \sin\omega \cdot \int_y^H c \cdot dy + f_D \qquad (14)$$

where f_D = the drag force exerted on the grains by the liquid over the depth (H-y), and the liquid component

$$\tau_f = \rho_f \cdot g \cdot \sin\omega \cdot \int_y^H (1-c) \cdot dy - f_D \qquad (15)$$

Furthermore, the granular normal stress balances the normal component of the submerged weight of grains above y,

$$\sigma_s = (\rho_s - \rho_f) \cdot g \cdot \cos\omega \cdot \int_y^H c \cdot dy \qquad (16)$$

EXPERIMENTAL DISTRIBUTIONS IN COLLISIONAL LAYER

Experiments

Bed-load transport experiments were conducted using lightweight granular materials in the laboratory tilting flume at the Czech Technical University in Prague. The flume and its measuring equipment are described elsewhere (Matoušek et al., 2016a). The experiments included detailed measurements of longitudinal velocity profiles over the flow depth using different measuring techniques (Pitot tube for liquid velocity, acoustic methods - Acoustic Doppler Velocity Profiler, Ultrasonic Velocity Profiler - for grain velocity). Furthermore, integral characteristics of the flow (flow depth and longitudinal slope, flow rates of both water and grains) were measured and vertical positions of interfaces in the layered structure of the flow were visually observed (photographed and filmed). We will consider results for one of the tested lightweight granular materials, the fraction of plastic cylinder-shaped grains (equivalent grain diameter d = 5.41 mm, ρ_s = 1307 kg/m^3, code TLT50).

Observed flow structure

Observed flows were steady-state quasi-uniform flows above the upper stage plane bed. The flows tended to be stratified (Figure 1) and composed of up to three distinct layers (water layer, collisional layer and dense sliding layer). The number of layers changed and the thicknesses of the particular layers varied with flow conditions (Matoušek et al., 2016b) depending on a value of the bed shear stress, τ_b, expressed in a dimensionless form as the bed Shields parameter,

$$\theta = \frac{\tau_b}{(\rho_s - \rho_f) \cdot g \cdot d}.$$

In most cases, the collisional layer (a layer of colliding grains with an approximately linear velocity profile, Figure 2) dominated over a dense sliding layer (the layer of grains sliding over each other and being in permanent contact with each other between the top of the stationary bed and the bottom of the collisional layer; note that the sliding velocity of grains was negligible compared to velocities in the collisional layer) and occupied a considerable part of the total flow depth H.

Visual observations and measurements of local velocities, u, allowed the layer interfaces to be identified. In Figure 2, the individual layers are identified thus: bed (deposit at positions $y/H < 0$), DL (dense layer), CL (collisional layer), WL (water layer). Figure 2 also shows how the layered structure varied with the bed Shields parameter θ. No DL was observed in TLT50-flows with θ lower than say 0.9.

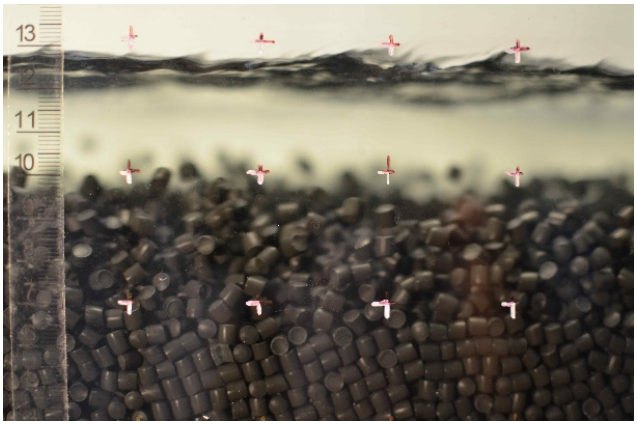

Fig. 1. Layered structure of flow with TLT50-grains (test run TLT50_20150713_3).

An analysis of measured bulk flux of grains and local velocities at the observed interfaces suggested that the local concentration at the bottom of the collisional layer, c_d, was smaller than the bed concentration, c_b, and varied with θ provided that a linear profile was assumed for concentration in CL (Matoušek et al., 2016b). For $\theta < 0.9$, c_d did not exceed approximately 0.47, the condition $c_d = c_b$ was reached at $\theta > 1$.

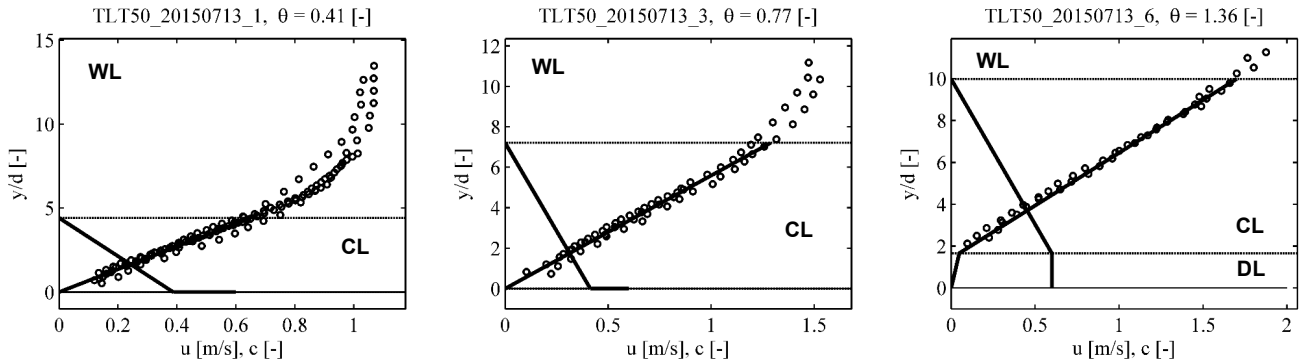

Fig. 2. Observed flow structure in laboratory flume. Legend*:* o = measurements of local velocity *u* (Pitot tube, Acoustic Doppler Velocity Profiler, Ultrasonic Velocity Profiler); horizontal thin lines = visually observed layer interfaces, DL = dense layer, CL = collisional layer, WL = water layer; thick lines = linear profiles of velocity and concentration based on analysis of experimental data.

DISCUSSION OF DISTRIBUTIONS

An evaluation of a vertical distribution of stresses in CL is pragmatically based on linear distributions of velocities and concentrations across CL. Besides the stress distribution, the evaluation enables stress conditions at the bottom of the collisional layer to be identified, i.e. at the interface with the bed layer, or DL. In this evaluation procedure, we neglect any possible side-wall effect on the stress distribution along a vertical axis of symmetry of the flume cross section.

Relevant information available from experiments

Information on the distribution of concentration (a linear *c*-profile across CL) enables one to determine the distribution of the total shear stress $\tau_e(y)$ across the entire flow depth H using Equation 13. Also available from the same experimental results is the distribution of the granular normal stress $\sigma_s(y)$ which may be extracted using Equation 16. Direct determination of the granular shear stress $\tau_s(y)$ from the momentum balance is not possible because the experiments provide no information about the local drag force (f_D in Equation 14). Available information on the distributions of c, u, and $\sigma_s(y)$ enable us to evaluate the distribution of local granular shear stress using the constitutive relations (Equations 1 and 2). The use of the momentum-based $\sigma_s(y)$ in Equation 1 produces a corresponding distribution of the granular temperature $T(y)$ and this used as an input to Equation 2 gives $\tau_s(y)$. Furthermore, the processed distributions of $T(y)$ and $\tau_s(y)$ enable evaluation of the distributions of fluctuation energy terms from the third constitutive relation (Equation 9).

Distribution of concentration-related functions

The distributions of G from Equation 3 for CKT and from Equation 8 for EKT are compared in Figure 3. The two distributions diverge considerably at $c > 0.47$, where G by EKT becomes more sensitive to c than G by CKT. In our experiments, the local concentration at the bottom of the collisional layer $c_d > 0.47$ only if the bed Shields parameter was higher than approximately 0.9.

The CKT functions f_σ, f_τ tend to infinity at $c = 0$ and thus their values are extremely sensitive to c in the range of low c values (Figure 4). However, they start converge to the limiting values of f_σ, f_τ given by EKT (i.e. for $c \to 1$) at c-values much smaller than 1. At the typical value of the bed concentration, $c_b = 0.60$, the difference in f-values between CKT and EKT is negligible and is thus considered negligible at $c = 0.47$ as well.

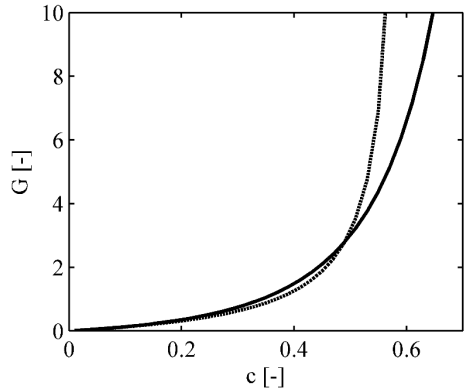

Fig. 3. Concentration-related function for constitutive relations. Legend: solid line = function in CKT (Equation 3); dashed line = function in EKT (Equation 8 for $c_f = 0.49$ and $c_c = c_b = 0.60$).

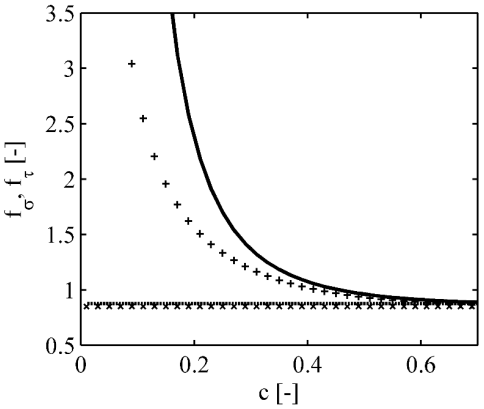

Fig. 4. Concentration-related functions for constitutive relations. Legend: solid line = function for normal stress in CKT (Equations 3–4); dashed line = function for normal stress in EKT (Equation 6 for $e = 0.7$); + = function for shear stress in CKT (Equations 3, 5); x = function for shear stress in EKT (Equation 7 for $e = 0.7$).

To summarize, Figures 3 and 4 show that the G-function is quite sensitive to c in the region of high c values, while f-functions become insensitive to c in the same region. Thus application of the EKT simplifications of the f-functions may not be necessary near the dense limit. On the other hand, the EKT simplification is applicable even if c is smaller than unity and it can simplify calculations at the bottom of CL. The EKT modification of G is essential for our test runs with $c_d > 0.47$, i.e. only for the runs with $\theta > 0.9$.

Distribution of granular temperature

The granular temperature is a key parameter of the kinetic theory as it occurs in all three constitutive relations. However, a direct measurement of the local T is extremely difficult and consequently its measurement is very rare in the literature (Sanvitale and Bowman, 2016).

We determine the distribution of T(y) for the experimentally based linear concentration distribution theoretically using a combination of Equations 1, 3, 4, and 16.

The distribution exhibits a maximum at a position within the collisional layer (Figure 5). T tends to zero at the top of CL and low values at the bottom of CL. In the lower part of CL, damping of T is due to high c which is responsible for a reduction of granular velocity fluctuations. This also explains why the flow of the highest local concentrations (the flow of θ = 1.36) exhibits smaller values of T including the maximum T(y) than the flow of θ = 0.77.

The variation of T with the y within the collisional layer may affect the local coefficient of restitution e and hence local values of granular stresses.

Distribution of shear stress

The procedure described above produces distributions of local granular stresses across the collisional layer. As a result of the CKT-based procedure, the granular component of the total shear stress increases with the depth within CL at the expense of the fluid component of the total shear stress (Figure 6). The fluid component becomes zero at the position where the curve of the total shear stress distribution and the curve of the granular shear stress distribution intersect. Predictions of $\tau_s(y)$ are not valid at positions below the point of intersection. Figure 6 shows that the position of the point of intersection agrees well with the position of the visually observed bottom of CL provided that c_d does not exceed approximately 0.47 (flows of θ = 0.41 and θ = 0.77). The negligible fluid shear stress is a reasonable assumption for the bottom of the collisional layer and so can be considered reasonable the predictions of the granular stress distributions by the CKT-based formula.

Figure 6 also shows (flow of θ = 1.36) that the curve of predicted granular stresses intersects with the curve of the total shear stress distribution at positions far above the bottom of CL if local concentration in the lower part of CL exceeds 0.47. The point of intersection corresponds with the position at which $c \approx 0.47$, i.e. the value for which the EKT simplifications of the constitutive relations (modifications of functions for G, f_σ, f_τ) are not required. Hence, an application of the modified EKT relations would not improve the results in the sense that it did not provide a position of the point of intersection nearer to the observed bottom of CL.

Distribution of fluctuation energy terms

Distributions of the three terms of the CKT constitutive relation for the collisional fluctuation energy based on earlier determined distributions of c, γ, T, and τ_s are plotted in Figure 7. The distributions suggest that the diffusion term varies very little throughout the collisional layer and although it is important near the top of CL, it is negligible at the lower part of CL if compared to the other two terms. Hence, virtually the entire collisional energy produced by shearing is dissipated in the collision in the lower part of the collisional layer, for the lower Shields-parameter flows.

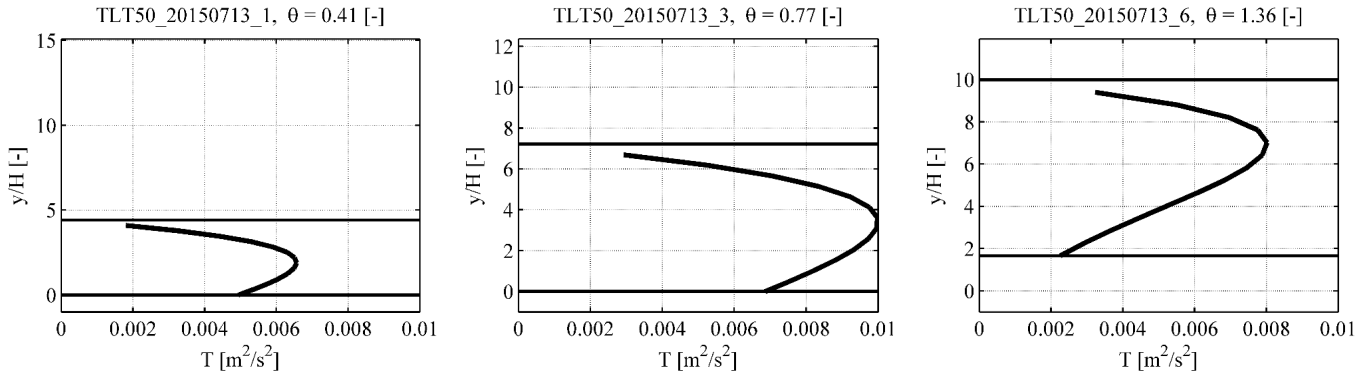

Fig. 5. Distribution of granular temperature in collisional layer. Legend: solid line = T using CKT (Equations 1, 4, 12); horizontal lines = layer interfaces.

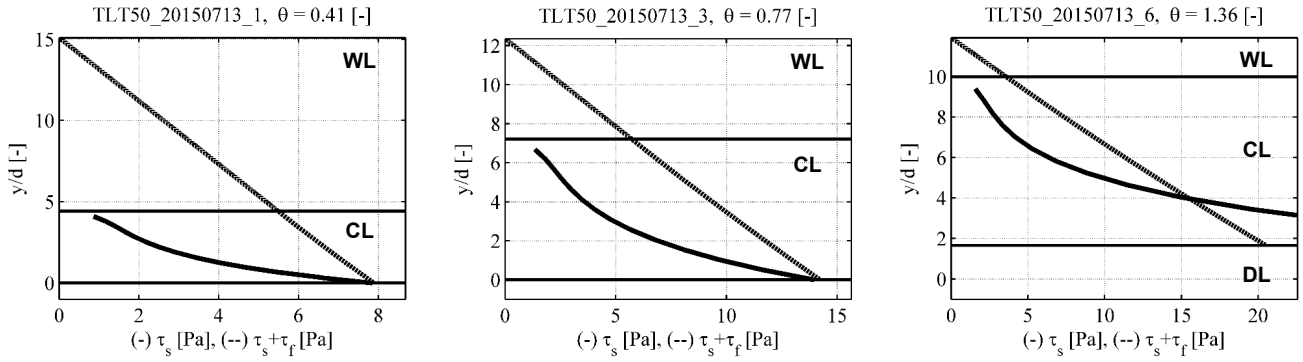

Fig. 6. Distribution of shear stresses in collisional layer. Legend: solid line = granular shear stress using classical kinetic theory (Equations 2, 6, 12); dashed line = total shear stress using momentum balance (Equation 13); horizontal lines = layer interfaces.

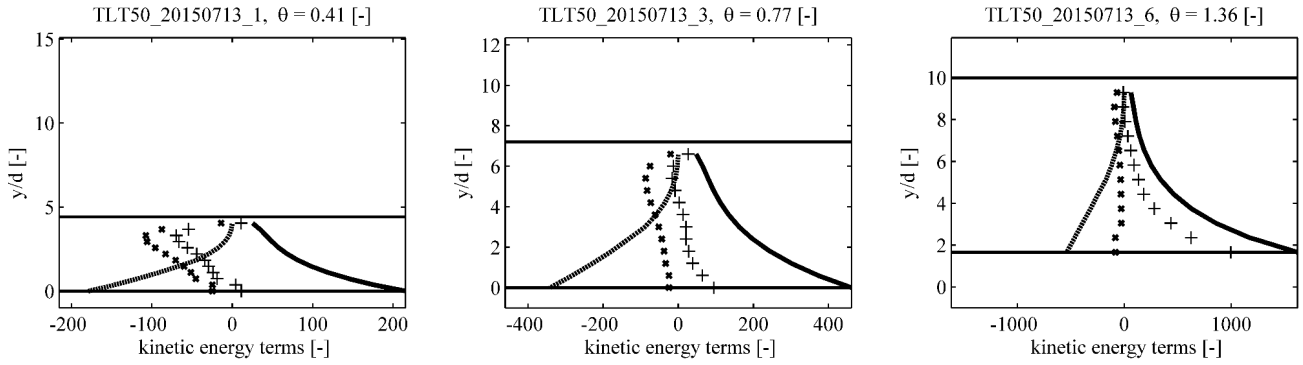

Fig. 7. Distribution of terms of fluctuation energy relation (Equation 9). Legend: solid line = production term (positive values); dashed line = dissipation term (negative values); x = diffusion term; + = sum of three terms; horizontal lines = layer interfaces.

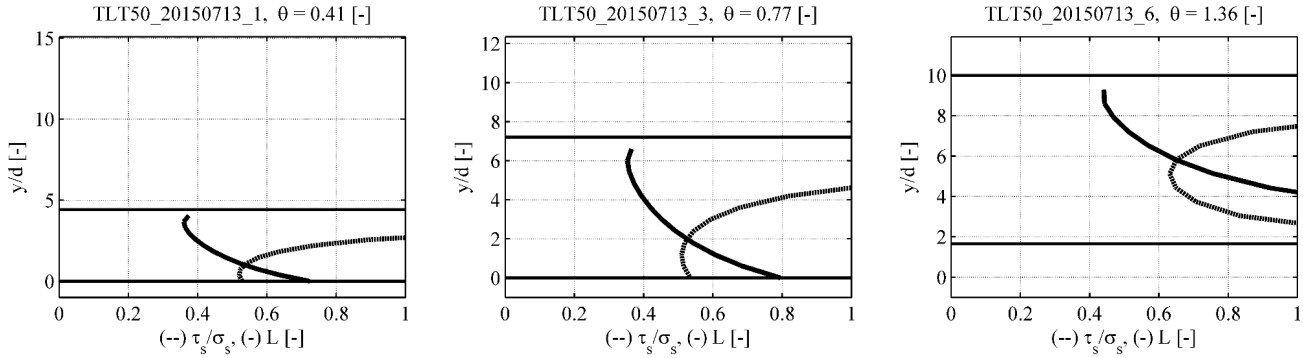

Fig. 8. Distribution of dimensionless correlation length and distribution of granular stress ratio in collisional layer. Legend: solid line = correlation length; dashed line = ratio of granular stresses; horizontal lines = layer interfaces.

However, this does not seem to be the case for the run with the largest Shields parameter (θ = 1.36) where the production is considerably higher than the dissipation at local concentrations exceeding approximately 0.47. Moreover, the relation does not find a balance among the three terms at $c > 0.47$ suggesting that the constitutive relation for CTK is not valid at positions of high c.

Evaluation of criteria/boundaries for application of constitutive relations

In Figure 8, the solid line gives a distribution of L (calculated by Equation 12 for a typical value of $C = 0.7$) across CL showing that L remains below the maximum value of 1 even at the bottom of CL for the two runs with $c_d < 0.47$. For the third run (θ = 1.36, $c_d = c_b$), $L > 1$ in the lower part of CL and L exceeds unity at the virtually same y-position as is the point of intersection of the distributions of the solids shear stress and the total shear stress (Figure 6). The local concentration $c \approx 0.47$ at this y-position.

In order to evaluate the limiting values of c delimiting the concentration range in which the constitutive relations can be applied, it is interesting to evaluate the distribution of the ratio of granular stresses by KT. Equations 1 and 2 give $\frac{\tau_s}{\sigma_s} = \frac{f_\tau}{4 \cdot f_\sigma} \cdot \frac{\gamma \cdot d}{\sqrt{T}}$ which leads to unrealistically high values of the stress ratio at low c (if $c \to 0$, then $T \to 0$ and $f_\tau / f_\sigma \to$ infinity). For the distributions of c and u simplified as linear profiles across the entire CL, the granular stress ratio reaches realistic values smaller than 1 at local c larger than approximately 0.18 only. Hence, this value is considered the minimum c for which the kinetic theory can be applied (provided that the distributions are assumed linear). At the bottom of CL, the ratio reaches a realistic value corresponding to a value of the Coulombic friction coefficient provided that the local L remains below 1 (i.e. for the two runs with $c_d < 0.47$). For the third run (θ = 1.36, $c_d = c_b$), the stress ratio values are realistic only in the range of y-positions corresponding with the range of c between approximately 0.18 and 0.47.

The correlation length L is related to the granular stress ratio by $L = 2 \cdot C \cdot \frac{f_\sigma}{f_\tau} \cdot \sqrt[3]{G} \cdot \frac{\tau_s}{\sigma_s}$. The term f_σ/f_τ by CKT increases from zero at $c = 0$ to 0.97 at $c = 0.47$ and remains approximately constant and equal to f_σ/f_τ by EKT at $c > 0.47$. At the y-position with $L = 1$ (and $c \approx 0.47$), the local ratio τ_s/σ_s is still lower than one (see Figure 8 for θ = 1.36). Hence, L exceeds unity due primarily to the extensive increase of G at the lower y-positions with $c > 0.47$. This is another indicator that $c = 0.47$ is a suitable upper limit for an application of the constitutive relations to the conditions considered in this work.

CONCLUSIONS

Constitutive relations of kinetic theory were tested in a collisional layer of intense bed load in a laboratory flume. Kinetic-theory based predictions of depth distributions of grain-related quantities (granular stresses, temperature and collisional energy) were evaluated using results of the bed-load experiments, assuming linear profiles of grain concentration and velocity across the collisional layer. The position of the bottom of the collisional layer resulting from the predicted distributions of shear stress agreed well with the experimentally observed posi-

tion if the local concentration at the bottom of the collisional layer did not exceed approximately 0.47. At positions with the local concentration bigger than 0.47 in the lower part of the collisional layer, the constitutive relations for shear stress and collisional energy failed no matter whether the classical form of the concentration-related functions or the simplified form associated with the extended kinetic theory were used in the constitutive relations. Hence, 0.47 is considered the upper limit of the local concentration of colliding grains to which the constitutive relations can be successfully applied in the conditions given by our experiment. The lower limit of local concentration appears to be approximately 0.18. This limit is based on the obtained distribution of the local ratio of collisional shear and normal stresses by the constitutive relations. The local granular stress ratio must be smaller than 1 and this is not satisfied at positions with $c < 0.18$ in the collisional layers of the observed flows.

Acknowledgement. The research has been supported by the Czech Science Foundation through the grant project No. 16-21421S. An assistance of V. Bareš, J. Hlom, J. Krupička, and T. Picek with obtaining the experimental results is highly acknowledged.

REFERENCES

Armanini, A., Capart, H., Fraccarollo, L., Larcher, M., 2005. Rheological stratification in experimental free-surface flows of granular-liquid mixtures. Journal of Fluid Mechanics, 532, 269–319.

Bagnold, R.A., 1954. Experiments on a gravity-free dispersion of large solid spheres in a Newtonian fluid under shear. Proceedings of Royal Society London, Series A, 225, 49–63.

Berzi, D., 2011. Analytical solution of collisional sheet flows. ASCE Journal of Hydraulic Engineering, 137, 10, 1200–1207.

Berzi, D., Fraccarollo, L., 2013. Inclined, collisional sediment transport. Physics of Fluids, 25, 106601.

Capart, H., Fraccarollo, L., 2011. Transport layer structure in intense bed-load. Geophysical Research Letters, 38, L20402.

Hunt, M.L., Zenit, R., Campbell, C.S., Brennen, C.E., 2002. Revisiting the 1954 suspension experiments of R. A. Bagnold. Journal of Fluid Mechanics, 452, 1–24.

Jenkins, J.T., Hanes, D.M., 1998. Collisional sheet flows of sediment driven by a turbulent fluid. Journal of Fluid Mechanics, 370, 29–52.

Matoušek, V., Krupička, J., Picek, T., 2013. Validation of transport and friction formulae for upper plane bed by experiments in rectangular pipe. Journal of Hydrology and Hydromechanics, 61**,** 2, 120–125.

Matoušek, V., Bareš, V., Krupička, J., Picek, T., Zrostlík, Š., 2016a. Experimental evaluation of bed friction and solids transport in steep flume. Canadian Journal of Chemical Engineering, 94, 1076–1083.

Matoušek, V., Bareš, V., Krupička, J., Picek, T., Zrostlík, Š., 2016b. Structure of flow with intense bed load layer. In: Proc. Int. Conf. River Flow 2016, Saint Louis, USA.

Sanvitale, N., Bowman, E., 2016. Using PIV to measure granular temperature in saturated unsteady polydisperse granular flows. Granular Matter, 18, 57.

Spinewine, B., Capart, H., 2013. Intense bed-load due to a sudden dam-break. Journal of Fluid Mechanics, 731, 579–614.

Torquato, S., 1995. Nearest-neighbor statistics for packings of hard spheres and disks. Physical Review E, 51, 4, 3170–3182.

Received 28 December 2017
Accepted 20 February 2018